

# CHAPTER 2

## THEORETICAL BACKGROUND

In this chapter, I will give a general review of the properties of semiconductors. Also, included in this chapter are the principles of operation and the electrical characteristics of solar cell.

### 2.1 Review of Semiconductor Properties

The aim of this section is not to treat the properties of semiconductors from fundamentals. Rather, it is to highlight those properties that are important in the operation of solar cells.

Semiconductors have an electronic structure such that one band of allowed states completely occupied by electrons is called the valence band ( $E_v$ ), which is separated by a forbidden energy gap ( $E_g$ ) from the next band of allowed states, the conduction band ( $E_c$ ). The conduction electrons are referred to electrons, which can move freely and carry electric currents. The removal of an electron from a nucleus leaves behind a hole. Electrons from neighboring atom can fill this hole and thus cause the hole to move to a new site. Therefore, the current flow in semiconductors is due to both motion of electrons in the conduction band and holes in the valence band.

#### 2.1.1 Energy Density of Allowed States

The number of allowed states per unit volume in a semiconductor is obviously zero for energies corresponding to the forbidden gap and nonzero in the

allowed bands. The expression of the number of allowed states per unit volume and energy,  $N_C(E)$ , at an energy  $E$  near the conduction band edge is given by <sup>1</sup>

$$N_C(E) = \frac{4\pi(2m_e^*)^{3/2}}{h^3} \sqrt{E - E_C} \quad (2.1)$$

where  $m_e^*$ : effective mass of the electron. A similar expression holds for energies near the valence band edge, so that

$$N_V(E) = \frac{4\pi(2m_h^*)^{3/2}}{h^3} \sqrt{E_V - E} \quad (2.2)$$

where  $m_h^*$ : effective mass of hole

## 2.1.2 Charge Carriers in Semiconductors

For the intrinsic semiconductor, the Fermi energy is near mid gap. The number of electrons in the conduction band per unit volume,  $n_0$ , at the thermal equilibrium is given by

$$n_0 = \int_{E_C}^{E_{C \max}} N_C(E) f(E) dE, \quad (2.3)$$

where  $f(E)$  is the Fermi-Dirac distribution and  $E_{C \max}$  is the top of the allowed conduction band.

Since  $E > E_C$ , and if  $(E_C - E_F) \gg kT$ , then  $(E - E_F) \gg kT$  hence the Fermi-Dirac distribution function reduces to the Boltzman distribution function,

$$f(E) = \frac{1}{1 + \exp\left[\frac{(E - E_F)}{kT}\right]} \cong \exp\left[\frac{-(E - E_F)}{kT}\right]. \quad (2.4)$$

Substituting Eq. (2.4) into Eq. (2.3) and replace the upper limit,  $E_{C \max}$ , by infinity, one obtains

$$n_0 = \int_{E_C}^{\infty} \frac{4\pi(2m_e^*)^{3/2}}{h^3} \sqrt{E - E_C} \exp\left[\frac{-(E - E_F)}{kT}\right] dE. \quad (2.5)$$

By changing the variable of integration to  $x = (E - E_C)/kT$ , Eq. (2.5) becomes

$$n_0 = \frac{4\pi(2m_e^*kT)^{3/2}}{h^3} \exp\left[\frac{-(E_C - E_F)}{kT}\right] \int_0^\infty x^{1/2} \exp(-x) dx. \quad (2.6)$$

The integral is the gamma function and equals  $\frac{1}{2}\sqrt{\pi}$ , Eq. (2.6) then becomes

$$n_0 = 2\left(\frac{2\pi m_e^* kT}{h^3}\right)^{3/2} \exp\left[\frac{-(E_C - E_F)}{kT}\right]. \quad (2.7)$$

One can define a parameter  $N_C$  as

$$N_C = 2\left(\frac{2\pi m_e^* kT}{h^2}\right)^{3/2}. \quad (2.8)$$

Hence,

$$n_0 = N_C \exp\left[\frac{-(E_C - E_F)}{kT}\right], \quad (2.9)$$

where  $N_C$  is called the effective density of states in the conduction band.

Similarly, the total number of holes in the valence band per unit volume can be written as

$$p_0 = N_V \exp\left[\frac{-(E_F - E_V)}{kT}\right], \quad (2.10)$$

where  $N_V = 2\left(\frac{2\pi m_p^* kT}{h^2}\right)^{3/2}$  which is called the effective density of states in valence band.

For an intrinsic semiconductor, the electrons concentration in the conduction band is equal to the holes concentration in the valence band. Hence, apply Eq. (2.9) and Eq. (2.10) to the intrinsic semiconductor, we can write

$$n_0 = n_i = N_C \exp\left[\frac{-(E_C - E_{Fi})}{kT}\right] \quad (2.11)$$

and

$$p_0 = p_i = N_V \exp\left[\frac{-(E_{Fi} - E_V)}{kT}\right], \quad (2.12)$$

where  $n_i, p_i$  are known as “the intrinsic carrier concentration”, which refers to the intrinsic electron and hole concentration, respectively.  $E_{Fi}$  is known as the intrinsic Fermi level.

Take the product of Eq. (2.11) and Eq. (2.12), we obtain

$$n_0 p_0 = n_i^2 = N_C N_V \exp\left[\frac{-(E_C - E_{Fi})}{kT}\right] \cdot \exp\left[\frac{-(E_{Fi} - E_V)}{kT}\right] \quad (2.13)$$

$$n_i^2 = N_C N_V \exp\left[\frac{-(E_C - E_V)}{kT}\right] = N_C N_V \exp\left(\frac{-E_g}{kT}\right). \quad (2.14)$$

The intrinsic Fermi-level position,  $E_{Fi}$ , can be given by

$$N_C \exp\left[\frac{-(E_C - E_{Fi})}{kT}\right] = N_V \exp\left[\frac{-(E_{Fi} - E_V)}{kT}\right],$$

$$E_{Fi} = \frac{1}{2}(E_C + E_V) + \frac{1}{2}kT \ln\left(\frac{N_V}{N_C}\right). \quad (2.15)$$

That means the Fermi-level in a pure and perfect semiconductor lies close to midgap and shifts from the band with the larger density of states in order to maintain equal numbers of electrons and holes.

For the extrinsic semiconductor, i.e., a semiconductor in which controlled amounts of impurity atoms were added. The thermal equilibrium electron and hole concentrations are different from the intrinsic carrier concentration. The Fermi energy may vary through the band gap energy, which will then change the value of  $n_0$  and  $p_0$  given by Eqs. (2.9) and (2.10). The change in the Fermi energy is a function of the donor or the acceptor concentration that are added to the semiconductor.

The equations for the thermal equilibrium electron and hole concentration can be written from Eqs. (2.9) and (2.10), then

$$n_0 = n_i \exp\left[\frac{E_F - E_{Fi}}{kT}\right], \quad (2.16)$$

$$p_0 = n_i \exp\left[\frac{-(E_F - E_{Fi})}{kT}\right]. \quad (2.17)$$

Eqs. (2.16) and (2.17) show that the Fermi-level changes from the intrinsic Fermi-level,  $n_0$  and  $p_0$  change from the  $n_i$  value. In n-type semiconductor,  $E_F > E_{Fi}$ , so that  $n_0 > n_i$  and  $p_0 < n_i$ ; thus  $n_0 > p_0$ . Similarly, in p-type semiconductor,  $E_F < E_{Fi}$  so that  $p_0 > n_i$  and  $n_0 < n_i$ ; thus,  $p_0 > n_0$ .

Consequently, the  $n_0 p_0$  product may be written as

$$n_0 p_0 = N_c N_v \exp\left[\frac{-E_g}{kT}\right]. \quad (2.18)$$

Eq. (2.18) is the same as Eq. (2.14) which is the case of an intrinsic semiconductor. So that,

$$n_0 p_0 = n_i^2. \quad (2.19)$$

However, the Eq. (2.19) was derived using the Boltzman approximation. If the Boltzman approximation is not valid, then, Eq. (2.19) is not valid.

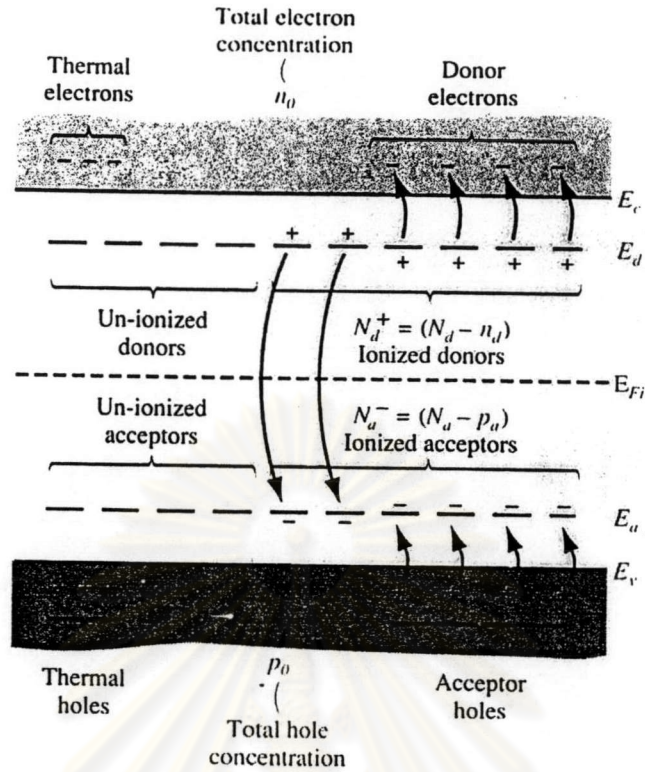
### 2.1.3 Compensated Semiconductors <sup>1</sup>

Figure (2.1) shows the energy band diagram of a semiconductor when both donor and acceptor impurity atoms are added to the same region. The charge neutrality condition is expressed by

$$n_0 + N_a^- = p_0 + N_d^+, \quad (2.20)$$

$$n_0 + (N_a - p_a) = p_0 + (N_d - n_d), \quad (2.21)$$

where  $n_0$  and  $p_0$  are the thermal equilibrium concentrations of electrons and holes in the conduction band and valence band, respectively.  $n_d$  is the concentration of electron in the donor energy states,  $N_d^+ = N_d - n_d$  is the concentration of positively charged donor states,  $p_a$  is the concentration of holes in the acceptor energy states, and  $N_a^- = N_a - p_a$  is the concentration of negatively charged acceptor states.



**Figure 2.1:** Energy band diagram of a compensated semiconductor showing ionized and un-ionized donors and acceptors <sup>1</sup>.

Assuming complete ionization,  $n_d$  and  $p_a$  are both zero, Eq. (2.21) becomes

$$n_0 + N_a = p_0 + N_d. \quad (2.22)$$

If we express  $p_0$  as  $n_i^2 / n_0$ , then Eq. (2.22) can be written as

$$n_0 + N_a = \frac{n_i^2}{n_0} + N_d \quad (2.23)$$

or

$$n_0^2 - (N_d - N_a)n_0 - n_i^2 = 0. \quad (2.24)$$

Hence,

$$n_0 = \frac{(N_d - N_a)}{2} + \sqrt{\left(\frac{N_d - N_a}{2}\right)^2 + n_i^2}. \quad (2.25)$$

Eq. (2.25) is used to calculate the electron concentration in an n-type semiconductor ( $N_d > N_a$ ). Although Eq. (2.25) was derived for a compensated semiconductor, this equation is also valid for  $N_a = 0$ .

Similarly, the hole concentration is given by

$$p_0 = \frac{(N_a - N_d)}{2} + \sqrt{\left(\frac{N_a - N_d}{2}\right)^2 + n_i^2}, \quad (2.26)$$

and is used to calculate the thermal equilibrium majority carrier hole concentration in a p-type semiconductor ( $N_a > N_d$ ). It also applies for  $N_d = 0$ .

The position of the Fermi energy level within the bandgap can be determined using Eq. (2.9).

Thus,

$$E_C - E_F = kT \ln\left(\frac{N_C}{n_0}\right), \quad (2.27)$$

where  $n_0$  is given by Eq. (2.25)

For n-type semiconductor in which  $N_d \gg n_i$ , then  $n_0 \cong N_d$ , thus

$$E_C - E_F = kT \ln\left(\frac{N_C}{N_d}\right). \quad (2.28)$$

If we have a compensated semiconductor, then we can replace  $N_d$  by  $N_d - N_a$ , or the net effective donor concentration.

For p-type semiconductor, from Eq. (2.10)

$$E_F - E_V = kT \ln\left(\frac{N_V}{p_0}\right). \quad (2.29)$$

If we assume that  $N_a \gg n_i$ , then Eq. (2.29) can be written as

$$E_F - E_V = kT \ln\left(\frac{N_V}{N_a}\right). \quad (2.30)$$

The expression for the relationship between the Fermi level and the intrinsic Fermi level given by

$$E_F - E_{Fi} = kT \ln\left(\frac{n_0}{n_i}\right), \quad (2.31 \text{ a})$$

$$E_{Fi} - E_F = kT \ln\left(\frac{p_0}{n_i}\right), \quad (2.31 \text{ b})$$

where the electron concentration,  $n_0$  and hole concentration,  $p_0$ , are given by Eqs. (2.26) and (2.27), respectively.

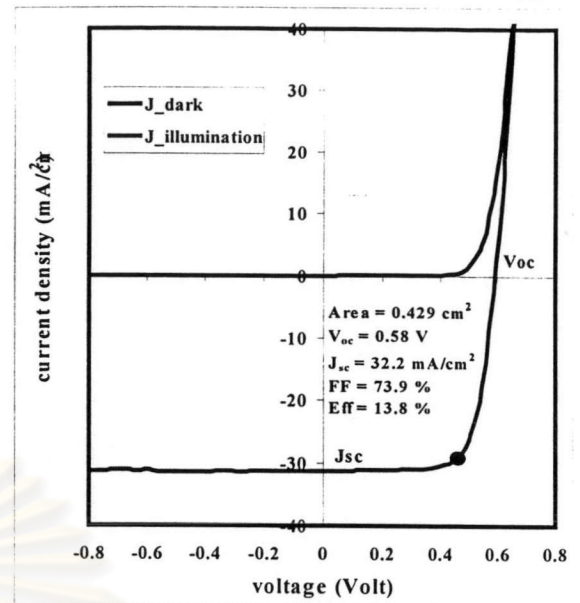
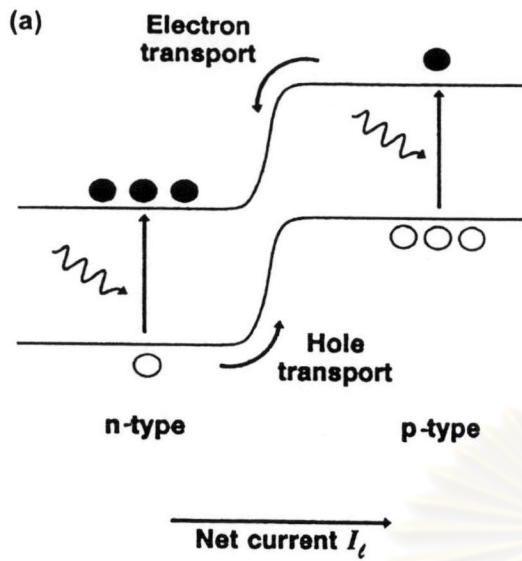
## 2.2 Solar Cell Operation

Simple model for the single junction solar cell is shown in Fig 2.2. In general, photons with an energy equal to or greater than the band gap are absorbed, creating electron-hole pairs. On the other hand, photons with the energy less than the band gap pass through the material and are not used for photovoltaic energy conversion.

Electrons and holes diffuse to a junction, either a p-n junction or some other type of junction where a strong internal electric field exists. Electrons and holes are separated by the field and give rise to electric voltage and current in the external circuit.

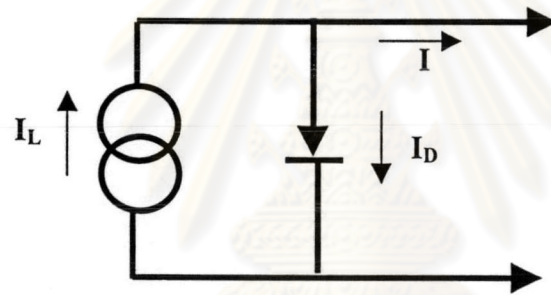
The I-V characteristic of a solar cell can be obtained by an equivalent circuit of the device shown in Fig. 2.2(c). Light-generated current  $I_L$  is represented by a current generator in parallel to a diode which represents the p-n junction.





(a)

(b)



(c)

**Figure 2.2:** (a) Schematic diagram showing current transport in a p-n junction under illumination. (b) Current-voltage characteristic curves of a solar cell in the dark and under illumination. (c) The equivalent circuit of a solar cell.

With the assumption that the current generated by light can be added to the current flow in the dark, so that the output current,  $I$ , can be expressed as <sup>2,3</sup>

$$I = I_0 \left[ \exp\left(\frac{qV}{kT}\right) - 1 \right] - I_L. \quad (2.32)$$

The first term of the right hand side of Eq. (2.32) is the forward current driven by voltage  $V$ ,  $I_0$  is often called the reverse saturation current,  $A$  is the diode

ideality factor that depending on the mechanism of the junction transport,  $k$  is the Boltzmann constant, and  $T$  is the temperature.

In evaluating a practical solar cell, four parameters of interest are the values of open-circuit voltage  $V_{oc}$ , the short-circuit current  $I_{sc}$ , the fill factor  $FF$ , and the conversion efficiency  $\eta$ .  $I_{sc}$  is equal to light-generated current  $I_L$ . The open-circuit voltage, corresponding to  $I = 0$  in Eq. (2.32), is given by <sup>2,3</sup>

$$V_{oc} = \frac{AkT}{q} \ln\left(\frac{I_L}{I_0} + 1\right). \quad (2.33)$$

The power output for any operating point in the fourth quadrant is equal to the area of the rectangle indicated in Fig. 2.2 (b). One particular operating point  $(V_{mp}, I_{mp})$  will maximize this power output. The fill factor  $FF$  is defined as <sup>2,3</sup>

$$FF = \frac{V_{mp} I_{mp}}{V_{oc} I_{sc}}. \quad (2.34)$$

It is a measure of how “square” the output characteristics are.

The energy-conversion efficiency  $\eta$  is then defined as <sup>2,3</sup>

$$\eta = \frac{V_{mp} I_{mp}}{P_{in}} = \frac{V_{oc} I_{sc} FF}{P_{in}}, \quad (2.35)$$

where  $P_{in}$  is the total power in the light incident on the cell.

## 2.3 Semiconductor Interfaces

There is an exchange of particles and energy whenever dissimilar materials are placed in intimate contact, which continues until thermodynamic equilibrium is established. This means that a flow of electrons, holes, and energy occurs across the interface until there is one electrochemical potential (Fermi level). The space charge (barrier or junction) region develops, which gives rise to an electrostatic potential

energy contribution across the interface. This potential energy developed across the space-charge region at the interface shifts the energy levels until their Fermi levels coincide, as in thermodynamic equilibrium (no bias, no light present).

The total built-in electrostatic potential energy  $V_0$  is related to the electrostatic field  $\xi_0$  existing in thermodynamic equilibrium;

$$V_0 = \int_{\text{interface region}} \xi_0 dx, \quad (2.36)$$

and

$$\frac{d}{dx}(\epsilon \xi_0) = \rho, \quad (2.37)$$

where  $\rho$  is charge density. Charge in delocalized band states and in localized gap states all contributes to  $\rho$  and, therefore, participates in shaping the electrostatic field region at an interface.

## 2.3.1 Semiconductor-Semiconductor Homojunctions

The general features of the semiconductor-semiconductor homojunction are the same semiconductor on either side of junction. Doping changes at interface either from n to p or from n<sup>+</sup> to n or p<sup>+</sup> to p.

### 2.3.1.1 Semiconductor p-n Homojunctions<sup>2</sup>

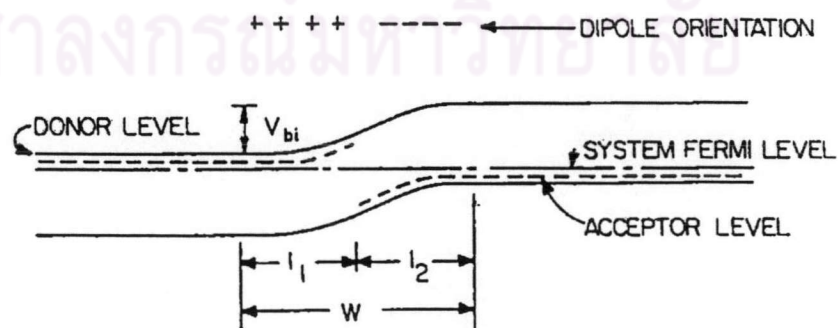


Figure 2.3: An n-p homojunction in thermodynamic equilibrium<sup>2</sup>.

Figure 2.3 shows an n-p homojunction in thermodynamic equilibrium. The built-in electrostatic potential energy is equal to the difference between the work functions,  $V_{bi} = \phi_p - \phi_n$ . The width of the space-charge region,  $w = l_1 + l_2$ , where  $l_1$  and  $l_2$  is the extent in the n-type and p-type material respectively. The quantities  $w, l_1, l_2$  and  $\xi = \xi(x)$  may be obtained by applying Poisson's equation to the interface region<sup>2</sup>. There are no interface states at the metallurgical junction because the homojunctions is made from diffusing one dopant into oppositely doped material. An analysis based on Poisson's equation yields

$$\xi_0 = \frac{eN_D(x + l_1)}{\epsilon_s} \quad ; \text{ for } -l_1 \leq x \leq 0, \quad (2.38)$$

and

$$\xi_0 = \frac{eN_A(l_2 - x)}{\epsilon_s} \quad ; \text{ for } -l_1 \leq x \leq 0. \quad (2.39)$$

The metallurgical junction is at  $x = 0$ . For a homojunction,  $\xi_0 = \frac{dE_C}{dx} = \frac{dE_V}{dx} = \frac{dE_{Fi}}{dx}$ , the total band bending is  $V_{bi}$  with  $E_{Fi}(x = -l_1) = 0$  and determined as a function of position from Eqs. (2.38) and (2.39).

$$E_{Fi} = \frac{eN_D x^2}{2\epsilon_s} + \left[ \frac{2N_D N_A e}{(N_A + N_D)\epsilon_s} V_{bi} \right]^{1/2} x + \frac{N_A}{N_A + N_D} V_{bi} \quad ; \text{ for } -l_1 \leq x \leq 0, \quad (2.40)$$

and

$$E_{Fi} = \frac{-eN_A x^2}{2\epsilon_s} + \left[ \frac{2N_D N_A e}{(N_A + N_D)\epsilon_s} V_{bi} \right]^{1/2} x + \frac{N_A}{N_A + N_D} V_{bi} \quad ; \text{ for } l_2 \geq x \geq 0. \quad (2.41)$$

When the p-n homojunction is biased by light or by a temperature gradient, then  $V_{bi}$  in Eqs. (2.40) and (2.41) becomes  $V_{bi} - V$ , where  $V$  is the change in the band bending across the junction. The p-n junction solar cell will be discussed latter in Chapter 3.

### 2.3.1.2 Semiconductor $n^+ - n$ ( $p^+ - p$ ) Homojunctions <sup>2</sup>

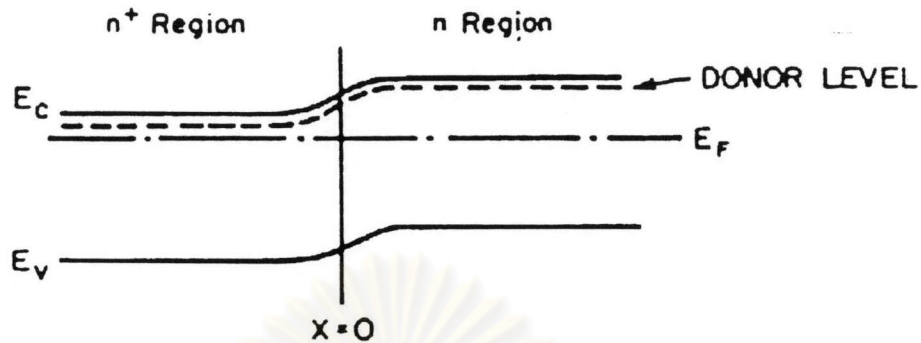


Figure 2.4: A high-low junction in thermodynamic equilibrium <sup>2</sup>.

Figure 2.4 shows  $n^+ - n$  homojunction and since the doping concentration in the  $n^+$  region is large, the total charge region will be of limited extent spatially. The photovoltage developed by such a junction is limited, due to lack of band bending (both sides are  $n$ -type) and due to lack of a substantial region over which conductivity can be modulated by light.

From Fig. 2.4, it is seen that the  $n^+ - n$  high-low junction forms a barrier which hinders minority carrier flows from the  $n$  to  $n^+$  regions. In solar cell structures, this has been used to reflect photogenerated minority carriers away from the high-low junction and toward some depleted barrier region where a large photovoltage can be developed.

### 2.3.2 Semiconductor-Semiconductor Heterojunctions

The general features of the semiconductor-semiconductor heterojunctions are different semiconductor on either side of the junction. If the doping changes type at the interface, the structure is referred to as being anisotype. Band bending is quite often dominated by interface states.

2.3.2.1 Anisotype Heterojunctions <sup>4</sup>

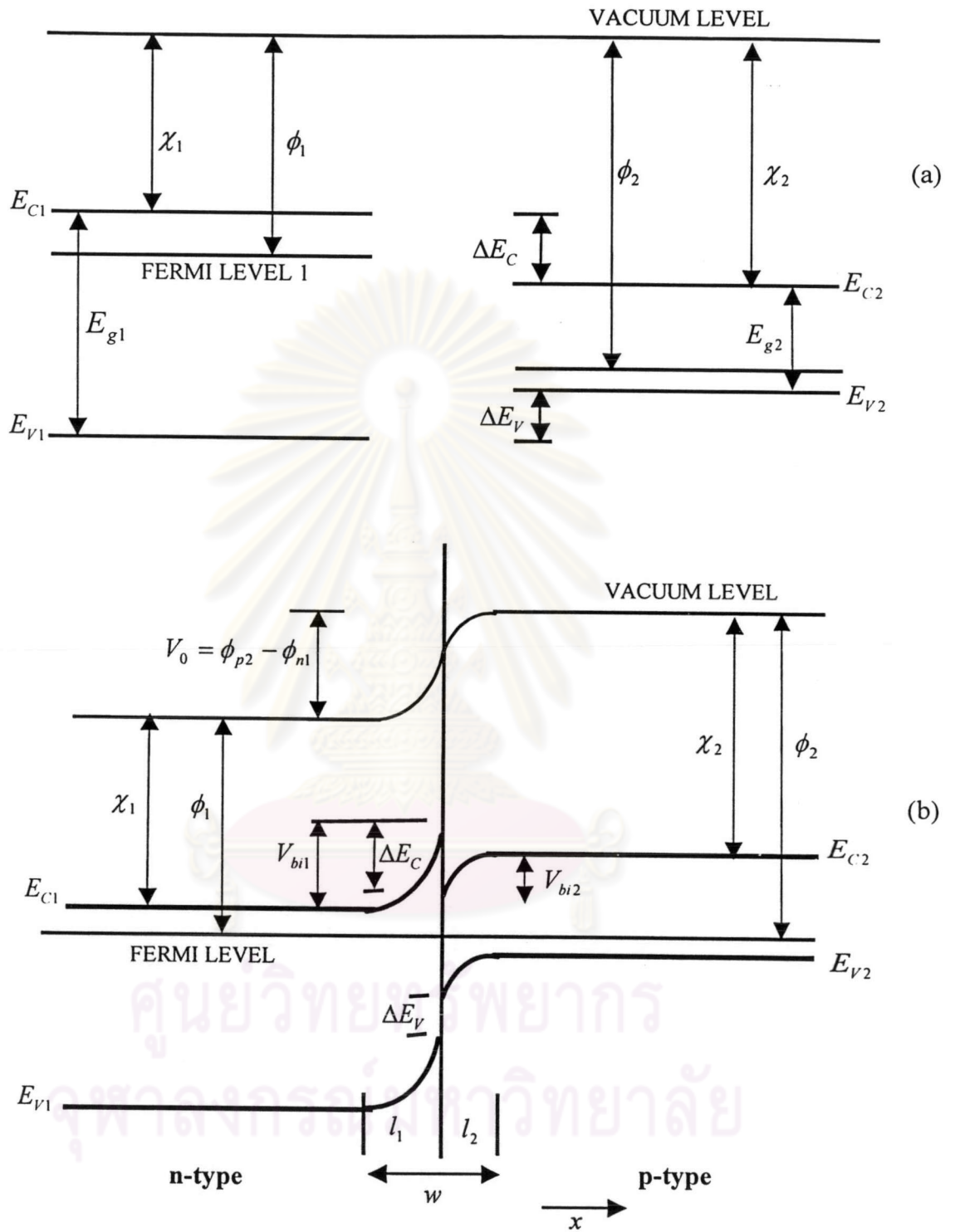


**Figure 2.5:** Equilibrium energy band diagrams before (a), and after (b) the formation of an abrupt n-p heterojunction in thermodynamic equilibrium. In this example, it is assumed that there are no interface states at  $x = 0$ , the metallurgical junction.

Figure 2.5 presents an ideal n-p (anisotype) heterojunction structure (Anderson model). It is assumed that there are no interface states. The n-type material has an electron affinity  $\chi_1$  and the work function is  $\phi_{n1} = \chi_1 + V_{n1}$ . The p-type material has an electron affinity  $\chi_2$  and the work function is  $\phi_{p2} = \chi_2 + E_{g2} - V_{p2}$ .

The band bending  $V_{bi1}$  in material 1 and the band bending  $V_{bi2}$  in material 2 represent the electrostatic potential energy required to equate the Fermi levels across this interface; i.e.,  $V_0 = V_{bi1} + V_{bi2}$ . Thus

$$V_{bi1} + V_{bi2} = \phi_{p2} - \phi_{n1} . \quad (2.42)$$

The discontinuity in the conduction band edge and in the valence band edge  $\Delta E_C$ , and  $\Delta E_V$  are

$$\Delta E_C = -(\chi_2 - \chi_1), \quad (2.43)$$

$$\Delta E_V = \chi_2 + E_{g2} - (\chi_1 + E_{g1}), \quad (2.44)$$

where  $\Delta E_C$  and  $\Delta E_V$  must be zero for the homojunctions.

The space charge width on each side and the band bending as a function of position are given by <sup>4,5</sup>

$$E_{Fi1} = \frac{e}{2\epsilon_{s1}} N_D x^2 + \frac{e}{\epsilon_{s1}} N_D I_1 x + \frac{e N_D I_1^2}{2\epsilon_{s1}} \quad ; \text{ for } -I_1 \leq x \leq 0, \quad (2.45)$$

and

$$E_{Fi2} = \frac{-e}{2\epsilon_{s2}} N_A x^2 + \frac{e N_A I_2 x}{2\epsilon_{s2}} \quad ; \text{ for } I_2 \geq x \geq 0. \quad (2.46)$$

where

$$I_1 = \left[ \frac{2\epsilon_{s1}\epsilon_{s2}N_A(\phi_{p2} - \phi_{n1})}{eN_D(\epsilon_{s2}N_A + \epsilon_{s1}N_D)} \right]^{1/2}, \quad (2.47)$$

$$I_2 = \left[ \frac{2\epsilon_{s1}\epsilon_{s2}N_D(\phi_{p2} - \phi_{n1})}{eN_A(\epsilon_{s2}N_A + \epsilon_{s1}N_D)} \right]^{1/2}, \quad (2.48)$$

The sum of  $I_1$  and  $I_2$  yields  $w$ . Also, from Eqs. (2.45) and (2.46), it follows that

$$V_{bi1} = \frac{eN_D I_1^2}{2\epsilon_{s1}}, \quad (2.49)$$

and

$$V_{bi2} = \frac{eN_A I_2^2}{2\epsilon_{s2}}. \quad (2.50)$$

The maximum electric field in the interface region is at  $x = 0$ . One obtains

$$\xi_{\max} = \frac{e}{\epsilon_{s1}} N_D I_1 = \left[ \frac{2eN_D V_{bi1}}{\epsilon_{s1}} \right]^{1/2}, \quad (2.51)$$

or

$$\xi_{\max} = \frac{e}{\epsilon_{s2}} N_D I_2 = \left[ \frac{2eN_A V_{bi2}}{\epsilon_{s2}} \right]^{1/2}. \quad (2.52)$$

Eqs. (2.45) - (2.52) characterize an ideal (Anderson) heterojunction in thermodynamic equilibrium. If the junction is biased by light, or by a temperature gradient, then the band bending in material 1 becomes  $V_{bi1} - V_1$  and that in material 2 becomes  $V_{bi2} - V_2$  replacing  $V_{bi1}$  and  $V_{bi2}$  in Eqs. (2.45) - (2.52).

For the case with no interface states,

$$N_D I_1 = N_A I_2, \quad (2.53)$$

$$(\epsilon_{s1} N_D (V_{bi1} - V_1))^{1/2} = (\epsilon_{s2} N_A (V_{bi2} - V_2))^{1/2}. \quad (2.54)$$

Also, the total change in the band bending  $V$  is

$$V = V_1 + V_2. \quad (2.55)$$

With Eqs. (2.54) and (2.55),  $V_1$  and  $V_2$  can simply be expressed in terms of the bias voltage  $V$ .

The spike in the conduction band in Fig. 2.5 (b) can affect the electron transport. If the junction were used as a solar cell, photogenerated electrons in  $I_2$ , and to the right, would tend to pile up at  $x = 0$  and then recombine at this plane. This would reduce the current generating effectiveness of the device.

For real heterojunctions, it is quite possible that the interface states will play a significant role in determining the junction configuration and it is quite possible that the change from one material to another will not be abrupt.



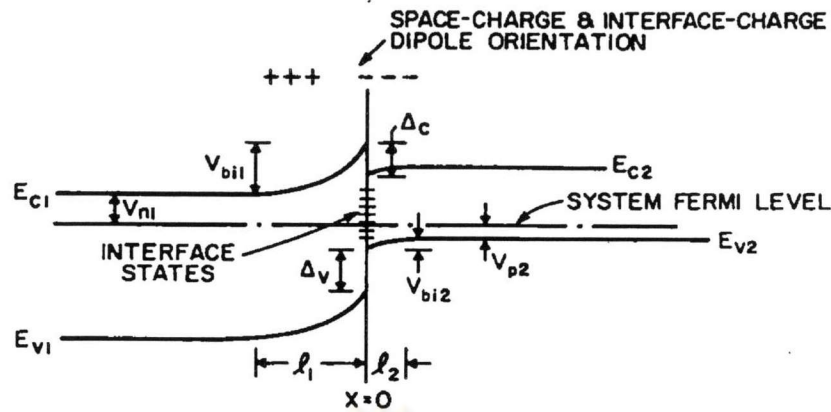


**Figure 2.6:** The n-p heterojunction of Fig. 2.5 but with interface states present. Junction is shown in thermodynamic equilibrium <sup>2</sup>.

Figure 2.6 is the same junction as Fig. 2.5 except for the presence of interface states at  $x = 0$ . The presence of interface states causes the change in size of the space-charge regions in each side. If the density of interface states is large enough, it is possible to have situations where the presence of these states acts to shield the semiconductors from one another. Essentially the interface states in these situations can develop any change necessary with a very small displacement of the Fermi level position at  $x = 0$  of Fig. 2.6. With the interface states present, a given  $V$  is distributed differently from it would be if there were no interface states. Localized gap states at the interface (arising from defects or impurities) can have a major influence on junction parameters in heterojunctions. The heterojunction solar cell will be discussed in more details in Chapter 3.

## 2.4 Trapping and Recombination

When electrons are excited to higher energy levels, they can return to a low-energy level by one of several recombination processes: (a) an electron can give up its energy through radiative recombination which involves emission of a photon; (b) an electron can give up its energy through Auger recombination, which involves the

transfer of its energy to another electron or hole; or (c) an electron can give up its energy by emission of a photon or phonons. Generally, this latter process will involve localized states existing in the bulk of a material, at surface, and at the grain boundaries.

### 2.4.1 Trapping

An allowed energy state, a trap, within the band gap may act as a recombination center, capturing both electrons and holes with almost equal probability. There are four basic processes, shown in Fig. 2.7, that may occur at this single trap.

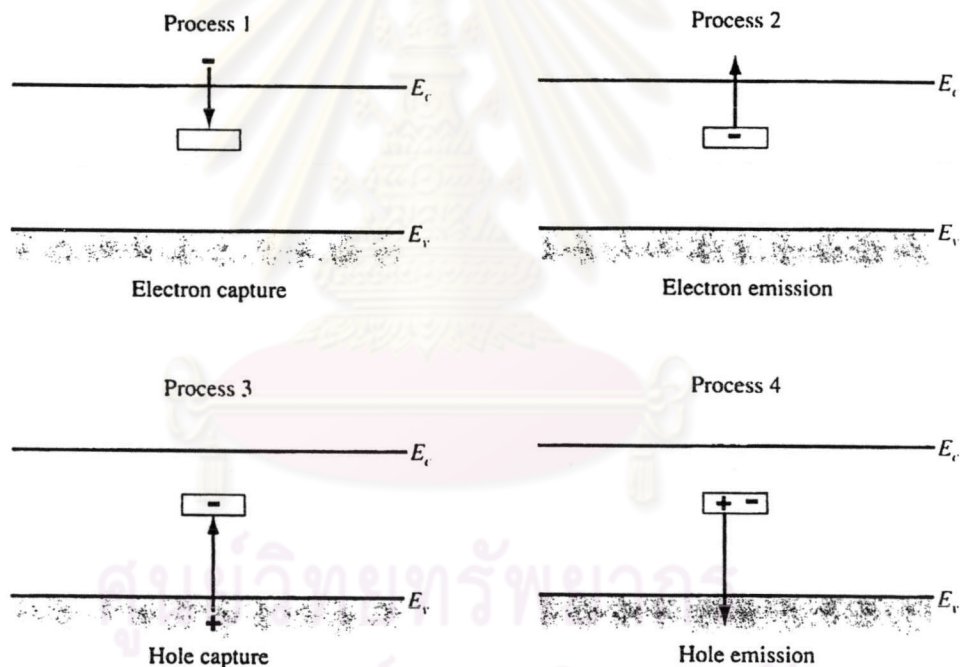


**Figure 2.7:** The four basic trapping and emission processes for the case of an acceptor-type trap<sup>1</sup>.

For example, an acceptor-type trap, the trap is negatively charged when it contains an electron and is neutral when it does not contain an electron. The four basic processes are as follows:

- Process 1: The capture of an electron from the conduction band by an empty trap.
- Process 2: The emission of an occupied electron from a trap level back into the conduction band.
- Process 3: The capture of the hole from the valence band by a trap containing an electron.
- Process 4: The emission of a hole from a neutral trap into the valence band.

### 2.4.2 Shockley-Read-Hall Recombination <sup>6</sup>

The net recombination rate from such trapping processes  $R$  depends on the localized gap states within the band gap. The recombination rate for a single level recombination center with energy  $E_t$  and concentration  $N_t$  is given by <sup>6</sup>

$$R = \frac{\sigma_n \sigma_p v_{th} (pn - n_i^2) N_t}{\sigma_n \left[ n + n_i \exp\left(\frac{E_t - E_{Fi}}{kT}\right) \right] + \sigma_p \left[ p + n_i \exp\left(\frac{E_{Fi} - E_t}{kT}\right) \right]}, \quad (2.60)$$

where  $\sigma_n$ ,  $\sigma_p$  are electron and hole capture cross section, respectively,

$v_{th} = \left(\frac{3kT}{m^*}\right)^{1/2}$  is the carrier thermal velocity,  $E_{Fi}$  is the intrinsic Fermi energy level,  $n_i$  is intrinsic carrier concentration, and  $n, p$  are electron and hole non-equilibrium concentration respectively.

The recombination rate is maximum when the recombination center or trap is located at the mid-band gap.

Under low level injection in p-type,  $n = n_{p0}$  and  $p \gg n \gg n_i$ , and the recombination center is located at the mid-band gap,  $E_t = E_{Fi}$ , then the recombination rate for electron is given by:

$$R_n = \sigma_n v_{th} N_t (n_p - n_{p0}) = \frac{n_p - n_{p0}}{\tau_{n0}}, \quad (2.61)$$

and for holes in p-type:

$$R_p = \sigma_p v_{th} N_t (p_n - p_{n0}) = \frac{P_n - P_{n0}}{\tau_{p0}}, \quad (2.62)$$

where  $n_p$  and  $p_n$  are the non-equilibrium concentration of electrons and holes respectively.  $n_{p0}$  and  $p_{n0}$  are the equilibrium concentration of electrons and holes, respectively.

The minority carrier lifetime for electron in p-type can be written as:

$$\tau_{n0} = \frac{1}{\sigma_n v_{th} N_t} \quad (2.63)$$

The minority carrier lifetime for electron in p-type can be written as:

$$\tau_{p0} = \frac{1}{\sigma_p v_{th} N_t} \quad (2.64)$$

Under high level injection conditions, the minority carrier lifetime for both holes and electrons in n-type and p-type can be expressed as

$$\tau_{p,n} = \tau_{p0} + \tau_{n0} \quad (2.65)$$

Under forward bias, the recombination rate can be written as <sup>6</sup>

$$R = \frac{\sigma_n \sigma_p v_{th} N_t n_i^2 [\exp(qV/kT) - 1]}{\sigma_n \left[ n + n_i \exp\left(\frac{E_t - E_{Fi}}{kT}\right) \right] + \sigma_p \left[ p + n_i \exp\left(\frac{E_{Fi} - E_t}{kT}\right) \right]} \quad (2.66)$$

## 2.5 Conclusions

In this chapter, I have given a brief review of semiconductor properties, semiconductor-semiconductor homojunction and heterojunction including the operation and electrical characteristics of solar cell.